Research in Astron. Astrophys. **2010** Vol. **10** No. **1**, 47 – 66
http://www.raa-journal.org *http://www.iop.org/journals/raa*

***R**esearch in*
***A**stronomy and*
***A**strophysics*

A new three-stage evolution model for millimeter to centimeter wavelength outbursts in BL Lacertae

Shan-Jie Qian[1,2], T. P. Krichbaum[2], A. Witzel[2], J. A. Zensus[2], Xi-Zhen Zhang[1], H. Ungerechts[3], H. D. Aller[4] and M. F. Aller[4]

[1] National Astronomical Observatories, Chinese Academy of Sciences, Beijing 100012, China; *rqsj@bao.ac.cn*
[2] Max-Planck-Institut für Radioastronomie, Auf dem Hügel 69, Bonn 53121, Germany
[3] Instituto Radioastronomia Milimétrica (IRAM), Avenida Divina Pastora 7, Núcleo Central, E-18012 Granada, Spain
[4] Department of Astronomy, University of Michigan, Ann Arbor, MI 48109-1042, USA

Received 2008 November 25; accepted 2009 May 7

Abstract The multi-frequency light curves of BL Lacertae during 1997.5 – 1999.5 have been modeled by four outbursts, each having a 3-stage evolution in the (S_m, ν_m) plane with distinct rising–plateau–decaying phases. It is shown that the observed light curves can be well fitted for the eight frequencies from 350 GHz to 4.8 GHz. The main characteristics of the model-fitting are: (1) the outbursts are found to have very flat spectra with an optically thin spectral index α (defined as $S_\nu \propto \nu^{-\alpha}$) of about 0.15. This is consistent with the results previously obtained by Valtaoja et al. (1992); (2) it is found that there is no spectral flattening between the rising–plateau phase and the decay phase. In other words, the optically thin spectral index does not change from the rising–plateau phase to the decay phase. These features are in contrast to the 3-stage shocked-in-jet model proposed by Marscher & Gear (1985) for submm–IR–optical flares, in which a spectral flattening of $\Delta\alpha = 0.5$ is predicted when a transition occurs from the Compton/synchrotron phase (or rising–plateau phase) to the adiabatic phase (or decay phase) with $\alpha \gtrsim 0.5$ for the shock being non-radiative. We propose a new model to interpret the fitting results, suggesting that the 3-stage evolution of the mm--cm outbursts in BL Lacertae may be related to the process of shock formation and propagation in a highly collimated jet (for example, a 'parabolic' jet). In particular, during the rising phase, the thickness of the synchrotron–radiating region created by the shock may rapidly increase with time (relative to the jet width) due to the rapid injection of relativistic electrons and a magnetic field, and this leads to the observed behavior that the turnover flux density S_m rapidly increases while the turnover frequency ν_m decreases. In the decay phase, the emitting plasma enters into a free expansion regime without further injection of relativistic electrons and a magnetic field (for example, when a transition from a collimated regime into a conical regime occurs). The plateau phase is a short period between the two regimes with no distinct features determined.

Key words: radio continuum: galaxies — radio outburst — quasars: individual: BL Lacertae

1 INTRODUCTION

Multi-frequency monitoring observations at cm–mm wavelengths have provided important information about the variability properties of blazars and the physical mechanisms of the emission processes. The studies of correlations (or evolutional relations) between cm–mm outbursts, IR–optical–UV flares and high-energy emissions (X-rays and γ-rays) are even more important for the understanding of the formation and evolution of the outbursts and flares (including acceleration/injection of high-energy electrons, location of emitting regions and radiation mechanisms, source dynamics and kinematics (relativistic bulk motion), etc.). Generally, it is believed that cm–mm and IR–optical–UV emissions (and some low-energy X-rays) are produced via the synchrotron mechanism. VLBI observations show that radio superluminal knots (ejection epoch obtained from the extrapolation of the knot's core distance to zero) emerge from the compact core following the associated optical (and gamma-ray) flares (for example, see Krichbaum et al. 1990a, 1998; Marscher 2005). Recently, through simultaneous polarization observations at optical and millimeter wavelengths (VLBI), it has been found that in some blazars optical flares could occur between the 3 mm and 7 mm VLBI pseudocores (D'Arcangelo et al. 2007; Jorstad et al. 2007; Marscher 2008). High-energy X-rays and γ-rays detected in strong blazars are believed to originate from inverse-Compton processes.

All the emissions from γ-ray to radio originate in the relativistic jets of blazars with the high-energy emissions in the innermost regions. Therefore, study of the correlations between the outbursts in the γ-ray, X-ray, optical and radio bands is essential to understanding the physics of the entire phenomenon occurring in the relativistic jets of blazars and the relationships between blazar activity and the black hole phenomenon.

Early in the 1970s, theoretical models (for example, see van der Laan 1966; Kellermann & Pauliny-Toth 1969) were already proposed to interpret the cm outbursts observed in blazars. Since then, many more models have been suggested. Generally, they can be divided into two major types: plasmon models and shock-in-jet models.

1.1 Plasmon Models

Plasmon models (both standard and generalized source expanding models) have the 3-dimensional adiabatic expansion of the plasmon as their main characteristic; at the same time, acceleration/injection of relativistic electrons, magnification/injection of magnetic fields and energy losses due to adiabatic expansion and synchrotron radiation are taken into account (Pauliny-Toth & Kellermann 1966; Peterson & Dent 1973; Pacholczyk & Scott 1976). These plasmon models can, in principle, explain the main properties of cm–mm outbursts of blazars: (1) the rapid increase of flux density (the rising phase of the outbursts) at high (optically thin) frequencies is interpreted as being due to the acceleration/injection of electrons and magnification/injection of magnetic fields, greatly increasing the emissivity of the plasmon; (2) the rising phases at lower frequencies which are delayed with respect to those at high frequencies is interpreted in terms of opacity effects with the plasmon becoming optically thin when moving from high frequencies to lower frequencies; (3) the declining phase is solely related to the adiabatic expansion of the plasmon. In addition, Qian et al. (1996c) explained the evolutional properties of the superluminal knot C4 of the quasar 3C345 in terms of a plasmon model, deriving its acceleration parameter.

Plasmon models have also been proposed to interpret mm–IR outbursts in which, during the growing phase, the turnover flux rapidly increases while the turnover frequency decreases. As suggested by Marscher & Gear (1985, in Appendix), for the mm–IR outburst in 3C273 during 1982 – 1983, if this phenomenon is related to Compton loss of relativistic electrons, the plasmon model requires some ad hoc parameters for the injection of a magnetic field and relativistic electrons. Thus, they concluded that shock-in-jet models are more plausible for interpreting mm–IR outbursts in blazars.

1.2 Shock-in-jet Models

Shock-in-jet models have long been applied to interpret cm–mm outbursts (both intensity and polarization variability) of blazars (for example, see Hughes et al. 1985, 1989a, b). In the shock-in-jet scenario, the evolution of cm–mm outbursts is explained in terms of a relativistic shock propagating outwards along the jet which causes continuous injection of emitting plasma (amplification/injection of the magnetic field and acceleration/injection of relativistic electrons). Some versions take into account the light-travel time effects of the consecutively injected plasma (O'Dell et al. 1988; Qian 1996a,b; Qian et al. 1997). However, in recent years, 3-stage evolutional models have been broadly applied to study the multi-frequency light curves and spectral evolution of cm–mm outbursts observed in blazars. Thus, we concentrate on describing these models and will apply this scenario to model-fit the multi-frequency light curves of the cm–mm outbursts observed in BL Lacertae below.

1.3 3-stage Evolutional Models

In the category of shock-in-jet models, the well known and most applicable model is the 3-stage evolutional model, which was originally proposed by Marscher & Gear (1985) to explain the evolution of a mm–IR outburst observed in 3C273 during 1982 – 1983. They show that after subtraction of the underlying quiescent level emission, the flare spectrum can be well fitted with a homogeneous synchrotron source. Its evolutional behavior can be described by three phases: growth (rising) phase, plateau phase and decay phase. The evolutional behavior can be distinctly described by the tracks in the (S_m, ν_m) plane (S_m and ν_m are the turnover flux and turnover frequency of the synchrotron spectrum). During the growth phase, the turnover flux density increases rapidly as the turnover frequency decreases. The plateau phase is a very short period in which the turnover flux density approximately remains constant with the turnover frequency continuing to decrease. During the decay phase, both the turnover flux density and turnover frequency decrease with time. These phases can be well described by the power-law relations of $S_m \propto {\nu_m}^{\epsilon}$ in the (S_m, ν_m) plane as the 3-stage evolution sketch shown in Figure 5 below.

Physically, Marscher & Gear assumed that in the case of a relativistic shock propagating along a conical jet, the jet plasma is adiabatically expanding, electrons are accelerated and the magnetic field is amplified via adiabatic compression by the shock front. The three phases of the 1982 – 1983 mm–IR outburst of 3C273 correspond to Compton–loss, synchrotron–loss and adiabatic expansion loss stages, respectively. That is, during the growth phase, the source is very compact and Compton loss dominates. Because Compton loss rapidly decreases with source expansion, the turnover flux density S_m rapidly increases while the turnover frequency ν_m decreases ($\epsilon \sim -3$). The plateau phase corresponds to the synchrotron stage when synchrotron loss dominates, and S_m slightly varies with ν_m, further decreasing ($\epsilon \sim 0$). The decay phase corresponds to the adiabatic expansion stage when expansion loss dominates, and the evolution of the outburst is like an adiabatically expanding plasmon ($\epsilon \sim +0.5 - 1$). In addition, during the Compton and synchrotron stage, the thickness of the shocked plasma (in a slab approximation) is proportional to the square root of the frequency ($x \propto \nu^{-\frac{1}{2}}$), and the optically thin spectral index at the Compton and synchrotron stages is equal to $s/2$ (the energy distribution of relativistic electrons is $N(\gamma_e) \propto {\gamma_e}^{-s}$ and $S_\nu \propto \nu^{-\alpha}$). In other words, there is spectral flattening of $\Delta\alpha = 0.5$ when the outburst transits from the Compton–synchrotron stage to the adiabatic stage.

Although the 3-stage evolution model was originally proposed by Marscher & Gear (1985) for a mm–IR outburst observed in 3C273, it has proved to be suitable to describe the variability behavior of cm–mm outbursts in blazars. Based on a statistical study of cm–mm outbursts for a group of blazars, Valtaoja et al. (1988, 1992) found that the spectra of the outbursts could be fitted with a simple homogeneous self-absorbed synchrotron source (with optically thick spectral index α (thick) = –2.5 and optically thin spectral index α (thin) = 0.2). This spectral shape persists throughout the

entire development of the outbursts; the only exception is a possible steepening of the optically thin spectra at high frequencies, indicating energy losses of high-energy electrons at later stages. The evolutional behavior of the outbursts can also be described by a 3-stage evolution in the (S_m, ν_m) plane (growing phase, plateau phase and decaying phase) with the turnover frequency ν_m decreasing with time. Recently, Stevens et al. (1995, 1998) analyzed the multi-frequency light curves of PKS 0420–014 and 3C273 and Litchfield et al. (1995) analyzed the multi-frequency light curves of 3C345. They both came to the conclusion that the 3-stage evolutional model (with rising–plateau–decay phases and power law S_m-ν_m relations) is applicable to the cm–mm outbursts observed in these sources. Thus, 3-stage evolution can be regarded as a common property of cm–mm outbursts in blazars. Rabaça et al. (1994) have explained the variability properties of a superluminal knot (C4 of 3C345) in terms of the 3-stage model.

However, we should point out that, although the 3-stage evolution pattern is applicable to describe the evolution behavior of cm–mm outbursts of blazars, its physical content is different from that of the original model proposed by Marscher & Gear (1985) for the mm–IR flare in 3C273. Firstly, in the evolution of cm–mm outbursts, there is no spectral flattening observed when the transition from the rising–plateau phase to the decay phase occurs. This is different from the MG model in which the flare spectrum flattens when the mm–IR flare transits from the rising--plateau (Compton–synchrotron) phase to the decay (adiabatic expansion) phase. Secondly, the optically thin spectral indices of the cm–mm outbursts are observed to be less than $\sim$0.5, which is inconsistent with the requirement of the MG model that the optically thin spectral index must be larger than 0.5 to keep the shock being non-radiative (for the mm–IR flare, the optically thin spectral index is $\sim$1.2). With these differences, we come to realize that the physical causes of the evolution of cm–mm outbursts in blazars are different from those of the Marscher & Gear model. In other words, the growth and plateau phases of cm–mm outbursts in blazars are not related to the Compton–synchrotron losses, but only to the adiabatic expansion loss.

In this paper, we will interpret the evolution of the cm–mm outbursts observed in BL Lacertae in terms of the 3-stage model and propose a new model to understand their physics.

2 MULTI-FREQUENCY LIGHTCURVES

In Figure 1, the multi-frequency flux density measurements of BL Lac are given at nine frequencies (5, 8, 15, 22, 37, 90, 150, 230 and 350 GHz) for the period from 1995.0 to 2000.5. The data at 5, 8 and 15 GHz are from the regular monitoring of the University of Michigan Observatory (Aller et al. 1999; Aller et al. 2003). The data at 22 and 37 GHz are from the Metsahovi flux density monitoring (Teräsranta et al. 2005). The data at 90, 150 and 230 GHz are from the regular flux density monitoring with the IRAM 30 m telescope (Ungerechts et al. 1998). It can be seen from Figure 1 that BL Lacertae has several outbursts with time scales of $\sim$0.5 yr. In the following, we will concentrate on analyzing the four outbursts during 1997 – 2000, which are clearly separated and have better multi-frequency data.

In Figure 2 is shown the optical flux density light curve (R-band). The optical data are from the optical quasar monitoring program at Colgate University (Balonek 2004), also previously published in Villata et al. (2004a) and Villata et al. (2004b).[1]

It is clear from Figure 2 that the optical flares consist of a number of peaks with timescales much shorter than those of the cm–mm outbursts. If the three consecutive cm–mm outbursts between 1997.4 and 1999.0 are respectively associated with the three optical flares (peaks) at $\sim$1997.48, $\sim$1998.15 and $\sim$1998.39, then it can be seen that the optical flares lead their associated radio–mm outbursts with timelags of $\sim 80 - 120$ d. These outbursts and also the optical flares have similar amplitudes. This property is different from that observed in the quasar-type blazar 3C454.3, in which Villata et al. (2006) recently found that for its cm–mm outbursts and optical flares observed in the

[1] The optical magnitude (m_R) is converted to optical flux density by using the formula $S_{\rm opt}$=$10^{-0.4m_R+3.479}$ (mJy).

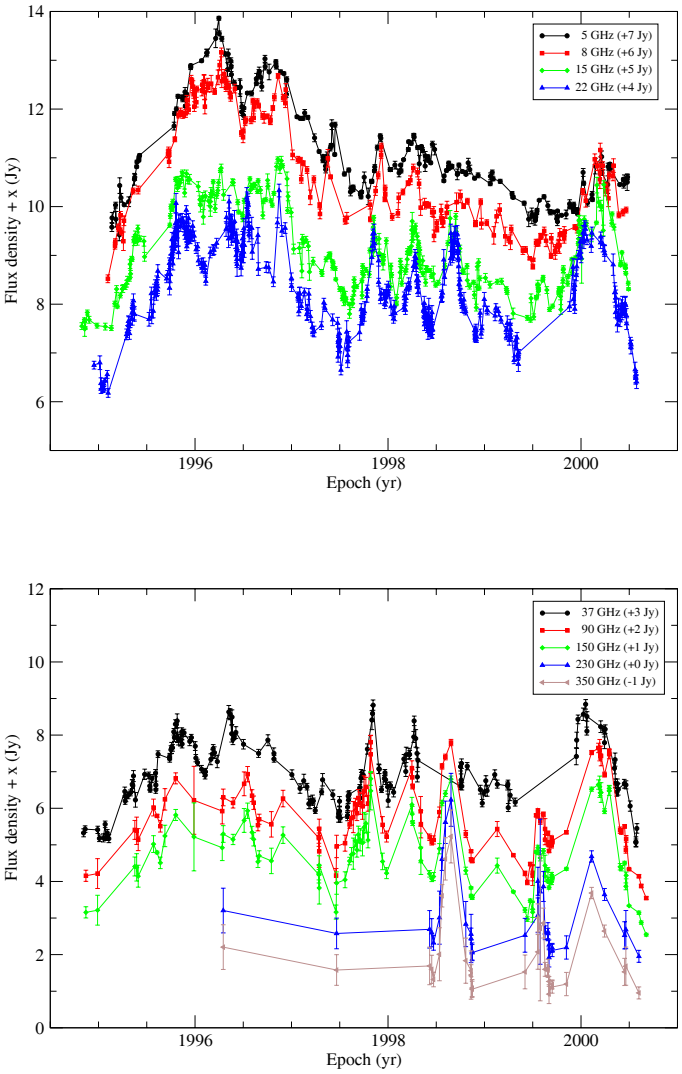

Fig. 1 Multi-frequency light curves of BL Lacertae during 1995 – 2000 at nine frequencies: 5, 8, 15, and 22 GHz (*upper*); 37, 90, 150, 230 and 350 GHz (*lower*). For better visibility, the data are shifted by arbitrary offsets, as indicated in the annotation for each frequency. The jagged lines through the data points are drawn solely to aid the eye to follow the variability.

2005 – 2006 period, the ratio of the amplitude of the delayed radio outbursts to the optical flares can vary significantly. This phenomenon is assumed to be caused by differential Doppler boosting for optical and radio flares and the rotation of the curved jet.

It can also be seen from Figure 1 (see also Figs. 6–12 below) that the 22 GHz and the mm light curves do not show noticeable timelags. This is a remarkably common feature of BL Lacertae objects (Stevens et al. 1994). In contrast, in radio-loud quasars (or blazar quasars) 22 – 37 GHz light curves often show significant timelags relative to the 90 – 350 GHz light curves.

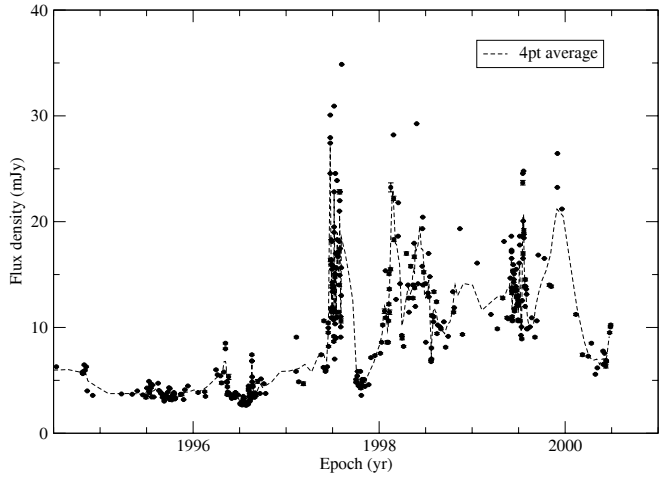

Fig. 2 Optical flux density light curve (R-band). The dashed line shows the 4-point running averages.

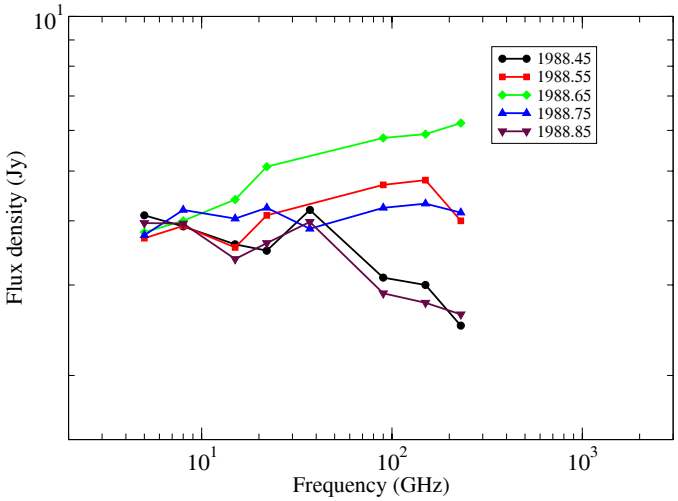

Fig. 3 Spectral evolution of the total flux spectrum of the flare during the period 1998.4 – 1998.9. Five spectra are shown for 1998.45 (*circle*), 1998.55 (*square*), 1998.65 (*diamond*), 1998.75 (*triangle-up*) and 1998.85 (*triangle-down*), respectively.

In Figure 3 is shown the spectral evolution of the total flux spectrum of the outburst (with the 230 GHz peak at ∼1989.62) for five epochs between 1998.45 and 1998.85. It has the general property of cm–mm outbursts observed in blazars: the outburst begins with the flux first increasing at higher frequencies and then propagating into lower frequencies. At epochs 1998.55 and 1998.65, the spectra were inverted and at epoch 1998.85, the outburst ended with the flux at high frequencies returning to its pre-outburst level.

3 MODEL-FITTING

3.1 Quiescent Spectrum

The adopted quiescent spectrum is listed in Table 1 and shown in Figure 4. The quiescent (or background) spectrum is chosen through a model-fitting procedure. We choose it by the following conditions: (1) the quiescent spectrum should be a flat spectrum between 3 cm and 3 mm in wavelength; (2) due to the superposition of the light curves of successive flares, we choose the background levels lower than the pre-flare and after-flare levels observed.

Table 1 Quiescent Spectrum

Frequency (GHz)	Flux density (Jy)
350	1.2
230	1.5
150	1.5
90	2.0
37	2.0
22	2.0
15	2.0
8	3.2
4.8	3.0

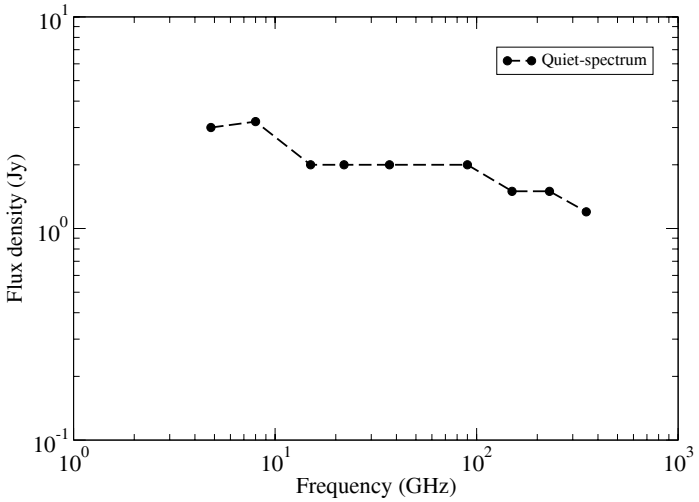

Fig. 4 Quiescent spectrum.

3.2 Scenario of Spectral Evolution

We will study the flux variations during the period 1997.5–1999.5. In the range of frequencies 4.8–350 GHz, there are apparently four peaks (or flares). However, the observations undersample the variations and we cannot directly derive the evolutionary track $S_m - \nu_m$. Therefore, we will use a 3-stage evolution model to fit the multi-frequency light curves. We will assume that the jet is adiabatic and the flaring regions are supplied by the injection of re-accelerated electrons and a compressed

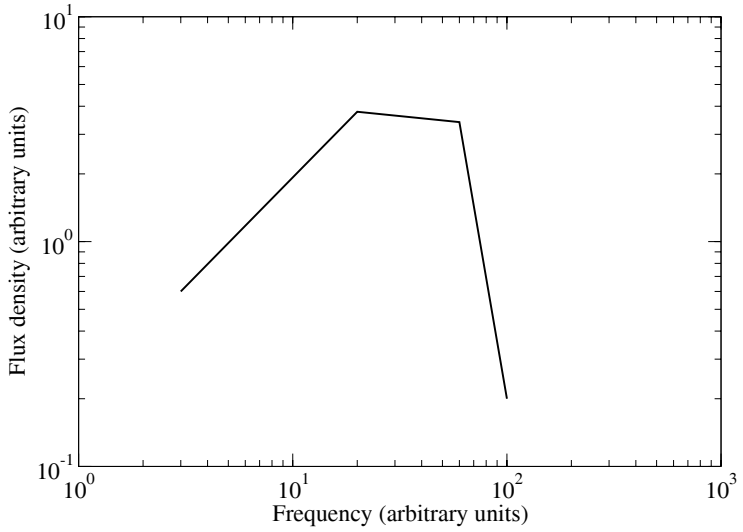

Fig. 5 A schematic plot showing the model of 3-stage evolution in the (S_m, ν_m) plane. The frequencies at the two breaks are ν_r and ν_f ($\nu_r > \nu_f$).

field by the propagating shocks to produce mm–cm flares. The scenario of 3-stage spectral evolution is described in Figure 5. Each flare has a common 3-stage evolution described as:

- Growth phase: $\nu_m = \nu_{m1}(\frac{t}{t_1})^{a_1}$, $S_m = S_{m1}(\frac{t}{t_1})^{b_1}$, and $S_m \propto {\nu_m}^{b_1/a_1}$;
- Plateau phase: $\nu_m = \nu_{m2}(\frac{t}{t_2})^{a_2}$, $S_m = S_{m2}(\frac{t}{t_2})^{b_2}$, and $S_m \propto {\nu_m}^{b_2/a_2}$;
- Decay phase: $\nu_m = \nu_{m3}(\frac{t}{t_3})^{a_3}$, $S_m = S_{m3}(\frac{t}{t_3})^{b_3}$, and $S_m \propto {\nu_m}^{b_3/a_3}$.

3.3 Model Parameters

We use four flares to fit the multi-frequency light curves, with their starting epochs at T_0 = 1997.5800, 1998.0044, 1998.4288 and 1998.7847, respectively.

The adopted quiescent spectrum is listed in Table 1 and shown in Figure 4. All the flares have the same values of (a_1, a_2, a_3) and (b_1, b_2, b_3). We assume the frequency of transition between the growth and plateau phases to be ν_r and that between the plateau and decay phases to be ν_f (Fig. 5).

For the four flares, we assume $\nu_r = 35\,\mathrm{GHz}$ and $\nu_f = 30\,\mathrm{GHz}$. The rising times (t_0) at which their turnover frequency reaches ν_r are adopted to be 70, 78, 70 and 115 days, respectively. The corresponding turnover flux densities (S_r) are 4.1, 3.6, 4.1 and 1.4 Jy respectively. In addition, following the results given by Valtaoja et al. (1988, from a statistical study of radio–mm flares) and Qian et al. (1998a, from a study of the γ–X-ray correlation of Mrk421), we assume a flat energy distribution of electrons, specifically a power-law index of $s = 1.3$ and, thus, the optically thin spectral index is $\alpha = 0.15$ ($S_\nu \propto \nu^{-\alpha}$).

Table 2 Model-fitting Parameters Used

	Flare-1	Flare-2	Flare-3	Flare-4
T_0	1997.5800	1998.0044	1998.4288	1998.7847
t_r(d)	70	78	70	115
ν_r(GHz)	35	35	35	35
ν_f(GHz)	30	30	30	30
S_r(Jy)	4.1	3.6	4.1	1.4
s	1.3	1.3	1.3	1.3
τ_m	0.12	0.12	0.12	012
a_1	–0.60	–0.60	–0.60	–0.60
a_2	–0.60	–0.60	–0.60	–0.60
a_3	–2.11	–2.11	–2.11	–2.11
b_1	1.5	1.5	1.5	1.5
b_2	0.07	0.07	0.07	0.07
b_3	–2.28	–2.28	–2.28	–2.28

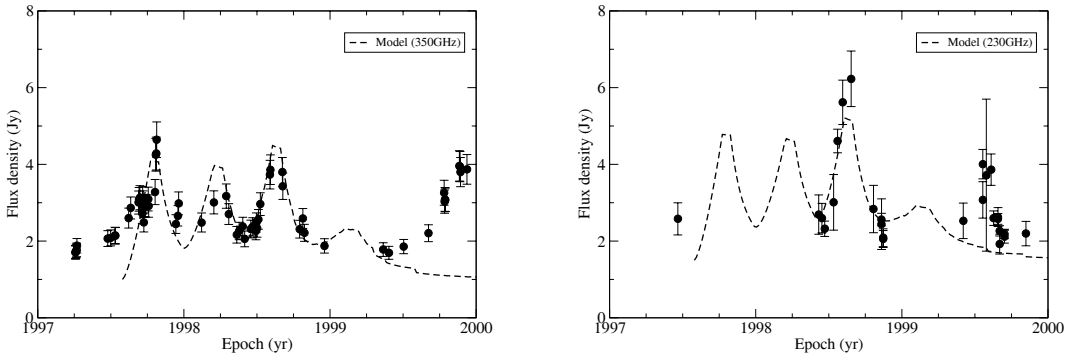

Fig. 6 Light curves at 350 GHz and 230 GHz.

3.4 Model-fitting Results

The theoretical light curves are calculated by using the standard formula for a uniform synchrotron source (Pacholczyk 1970):

$$S_\nu = S_m \frac{J(s, \frac{\nu}{\nu_1})}{J(s, \frac{\nu_m}{\nu_1})}, \tag{1}$$

where (S_m, ν_m) are defined by the 3-stage spectral evolution scenario described above. Also, ν_1 is the frequency at which the optical depth of the source is equal to unity: $\nu_1 = \nu_m {\tau_m}^{2/(s+4)}$. All the parameters adopted for model-fits of the four flares are summarized in Table 2. The results of the model-fittings are shown in Figures 6–10 by dashed lines and the observational data are shown by filled circles.

It can be seen that the variations during the period can be well fitted by the 3-stage evolution model with the same parameters (a_1, a_2, a_3) and (b_1, b_2, b_3) (same variation pattern), but the four flares have different amplitudes and timescales. A significant feature of the fitting is that during the 3 stages, the optically thin spectral index is the same, that is, we do not find any evidence for spectral flattening. In fact, due to the power index of the electron energy distribution being $s = 1.3$, any spectral flattening after the plateau phase is impossible.

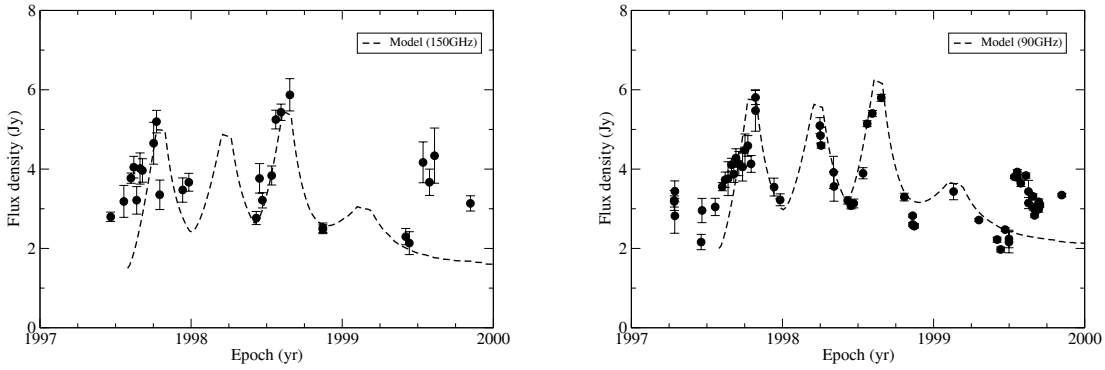

Fig. 7 Light curves at 150 GHz and 90 GHz.

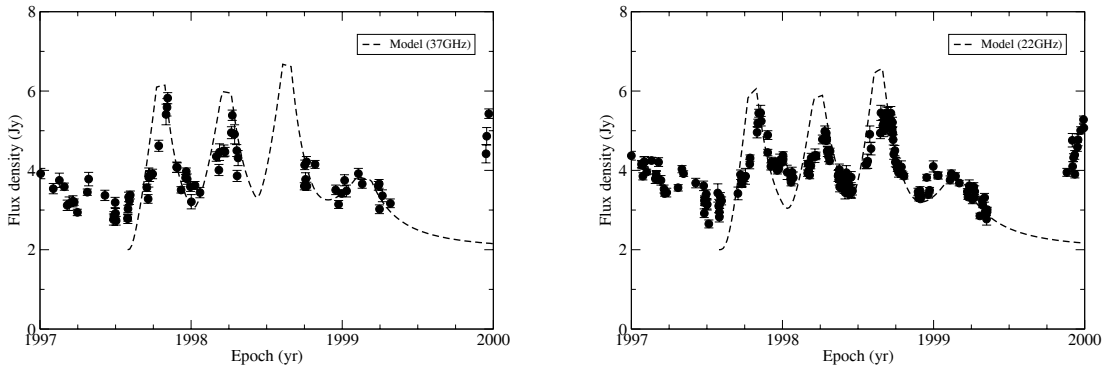

Fig. 8 Light curves at 37 GHz and 22 GHz.

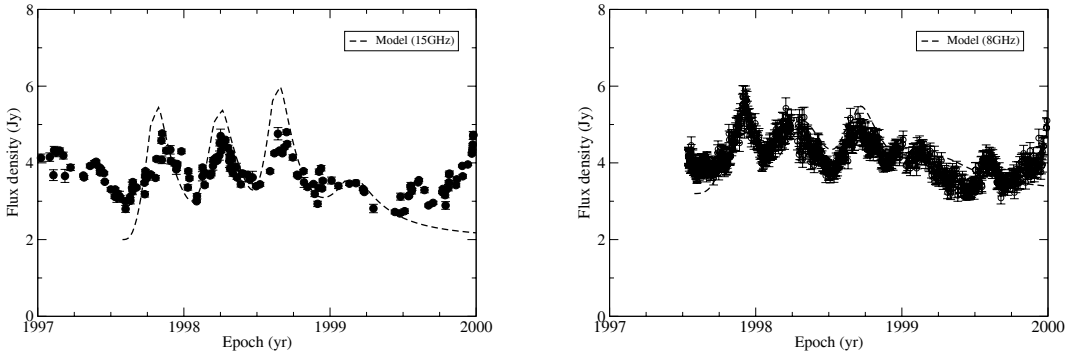

Fig. 9 Light curves at 14.5 GHz and 8 GHz.

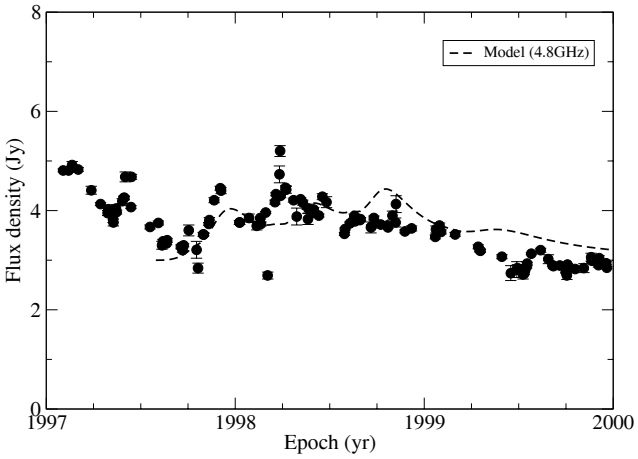

Fig. 10 Light curve at 4.8 GHz.

3.5 Light Curves

Taking into account the serious undersampling of the observations, our model-fitting results are generally good, especially at higher frequencies: for example, for the third flare, the four light curves at 350, 230, 150 and 90 GHz are well fitted by the model (see Figs. 6 and 7).

At lower frequencies (see Figs. 8 and 9), the model-fitting becomes a bit worse: the peak amplitudes obtained at 22 and 15 GHz by model-fitting are significantly higher than the observed ones. This could simply be due to the adopted background levels at the two frequencies being too high and a reduction of $\sim$0.5 Jy of the adopted background levels could better fit the first three flares. It is interesting that at 8 GHz the model-fitting is good.

3.6 Timelags

We have also determined the time delays of the cm–mm outbursts with respect to their respective optical flares (relative to the recorded optical maxima). These are shown in Figures 11–12. It is interesting to point out that the mm-flares are optically thin from the beginning, although they are delayed with respect to optical flares. This fact is consistent with the optically thin spectral index being less than $\sim 0.2 - 0.3$. How to explain the relationship between the optically thin mm-flares and their associated optical flares is worth further study, because this is different from the usually observed pattern of radio outbursts which are delayed with respect to the associated optical flares due to their opacity. It is possible that geometrical effects could explain this mm-delay. For example, the mechanism of jet-nozzle precession suggested by Stirling et al. (2003) for BL Lacertae could produce this kind of mm-delay, if the mm-emission region and the optical emission region are separated along the jet with a helical structure, each having a different Doppler boosting. However, in this scenario, the evolution of the mm–radio outbursts themselves is difficult to explain.

An alternative and plausible explanation might be that the optical flares occur in a region behind the VLBI mm-core, thus the optically thick phase of the mm-outbursts is not observed due to absorption by the jet plasma; only when the shock escapes from the mm-core can the outbursts be observed; then the mm-outbursts are optically thin from the beginning, but are delayed with respect to the optical flares. Recently, D'Arcangelo et al. (2007) found that optical flares in PKS 0420 – 014 occurred in the standing conical shock region of the jet between the 3 mm and 7 mm emitting

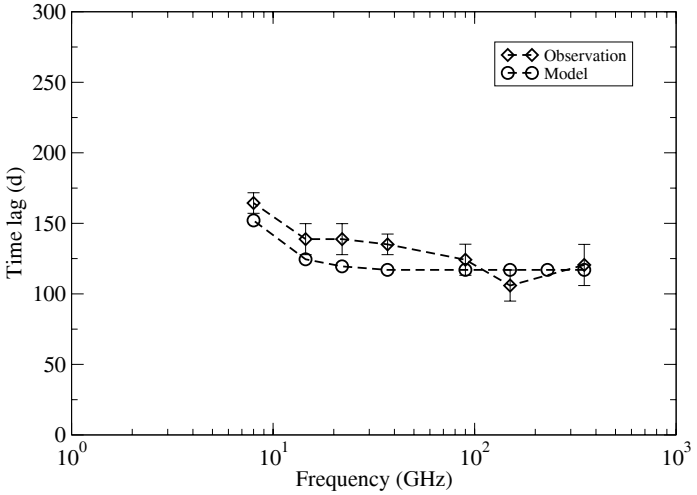

Fig. 11 Time lags of the first cm–mm outburst (peaking at 1997.81 at 350 GHz) with respect to the associated optical flare (peaking at 1997.48). Diamond–observation; circle–model.

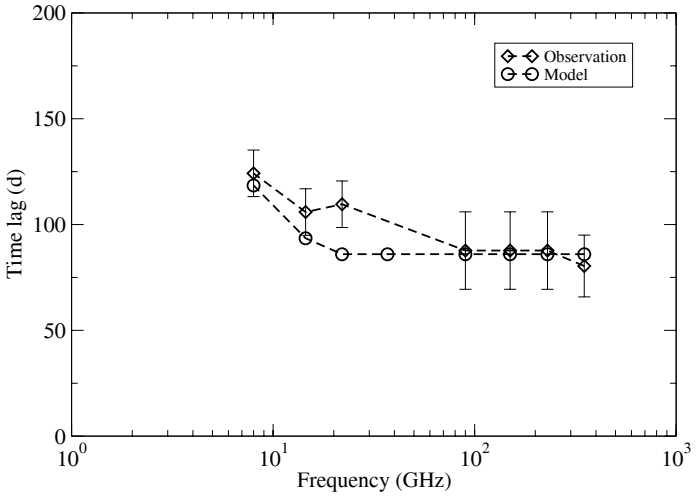

Fig. 12 Time lags of the third cm–mm outburst (peaking at 1998.62 at 230 GHz) with respect to the associated optical flare (peaking at 1998.39). Diamond–observation; circle–model.

regions (cores) and this fact can be regarded as an explanation for the optically thin mm-outburst delay compared to the optical flares in BL Lacertae here.

It can be seen from the figures that the effects of opacity in BL Lacertae occur at quite low frequencies (lower than $\sim$37 GHz). This is in contrast to those in flat-spectrum radio quasars (FSRQs) in which delays occur at much higher frequencies ($>$90 GHz).

4 INTERPRETATION

4.1 General Remarks

We have already pointed out that mm–radio outbursts in blazars often have ν_m (turnover frequency) decreasing with time. This implies that adiabatic expansion is its main characteristic even during their growth phase. The evolutional patterns of mm–radio outbursts have been studied in terms of shock-in-jet models. In the case of 3-dimensional adiabatic expansion (the jet itself expands sideways and the shocked plasma additionally expands along the jet axis), the energy distribution of the relativistic electrons ($N_*(\gamma_e)$) and the magnetic field strength (B_*) are usually represented by power laws in the flow's frame as follows.

$$N_*(\gamma) = N_{0*}\Big(\frac{r}{r_0}\Big)^{-(s+2)}{\gamma_e}^{-s}, \tag{2}$$

and

$$B_* = B_{0*}\Big(\frac{r}{r_0}\Big)^{-a}, \tag{3}$$

where γ_e is the Lorentz factor of an electron, r is the jet radius, N_{0*} and B_{0*} are the values at $r = r_0$ (r_0 is usually assumed to be the radius at the base of the jet (or nozzle)), s ($\equiv 2\alpha$+1) is the energy spectral index (α is the spectral index). (Note: in 3-dimensional adiabatic expansion, the power-law index of the electron energy distribution is proportional to $r^{-(s+2)}$, instead of $r^{-\frac{2}{3}(s+2)}$ as in the case of 2-dimensional adiabatic expansion; see Marscher & Gear 1985.) In the slab approximation and using the standard theory of a uniform synchrotron source, we have

$$S_\nu \propto N_{0*}{B_{0*}}^{\frac{s+1}{2}} r^2 x_\nu \nu^{\frac{1-s}{2}} \delta^{\frac{s+3}{2}}, \tag{4}$$

$$S_m \propto {N_{0*}}^{\frac{5}{s+4}} {B_{0*}}^{\frac{2s+3}{s+4}} {x_m}^{\frac{5}{s+4}} r^2 \delta^{\frac{3s+7}{s+4}}, \tag{5}$$

$$\nu_m \propto {N_{0*}}^{\frac{2}{s+4}} {B_{0*}}^{\frac{s+2}{s+4}} {x_m}^{\frac{2}{s+4}} \delta^{\frac{s+2}{s+4}}, \tag{6}$$

where we include the beaming effects (Doppler factor δ), which indicates that both intrinsic variation and change of Doppler factor should be considered normally. S_m and ν_m are the turnover flux and turnover frequency of the synchrotron spectrum of the shocked plasma. Moreover, δ is the Doppler factor of the emitting region, S_ν is the flux density at an optically thin frequency ν, and x_m (x_ν) is the size of the emitting region along the line-of-sight at the turnover frequency (at an optically thin frequency) in the observer's frame. Here, we would not specify the relation between r and d, the distance from the apex along the jet: for example, in the case of a conical jet $r \propto d$, but in collimated jets it could be proportional to $d^{1/q}$ ($q \gg 1$, see below).

We have shown that, for interpreting mm–cm outbursts in blazars and applying the 3-stage evolution model, the following observed characteristics and their differences from the sub-mm–IR outbursts discussed by Marscher & Gear (1985) should be taken into account:

- The optically thin spectral indices of cm–mm outbursts are usually less than 0.5. They do not change throughout the evolution of the outbursts, except for possible spectral steepening during the decay phase at mm-wavelengths;
- Although the S_m–ν_m evolution pattern can be described by a 3-stage model similar to Marscher & Gear's model, there is no spectral flattening when the transition from the rising–plateau phase to the decay phase occurs.
- Growth phase of mm–cm outbursts is not related to the Compton stage of the MG's model.

The above characteristics of cm-mm outbursts have been indicated by several authors (Qian et al. 1997, 1998a,b; Litchfield et al. 1995; Stevens et al. 1995, 1996). These properties clearly show that

for cm–mm outbursts, radiative losses (Compton and synchrotron) do not dominate; the dominating factors are adiabatic expansion, electron acceleration and field magnification. However, the applicability of the 3-stage evolution scenario clearly indicates that there must be some mechanism (instead of Compton and synchrotron radiative losses) at work to make the evolution of the growth–plateau phase superficially similar to that in the Marscher–Gear's model.

4.2 Generalized Models in the Shock-in-jet Scenario

In order to explain cm–mm outbursts which have a 3-stage evolution pattern similar to that for sub-mm–IR outbursts in MG's model, we will try to change the assumptions about the electron acceleration and field magnification in the shock-in-jet models. Obviously, all these assumptions can be modified. For example, more effective processes for electron acceleration and field amplification could also create rising–plateau phases for cm–mm outbursts (for example, in Pacholczyk–Scott's model (1976) for cm–mm outbursts, both induced and statistical acceleration and induced field amplification are applied). As Valtaoja et al. (1992) and Stevens et al. (1998) have suggested, cm–mm outbursts are caused by shock formation, in which the processes of electron acceleration and field amplification may be quite different from those adopted in Marscher & Gear's model (1985) and would assume $B \propto r^{-a}$ and $K \propto r^{-b}$ with a and b as free parameters to be derived for specific outbursts. (In MG's model, $a = 1$ (perpendicular field) or 2 (parallel field) and $b = 2(s+2)/3$.)

Therefore, in the case of an adiabatic expansion regime, we have for both rising and decaying phases:

$$\nu_m \propto r^{-\frac{2b+a(s+2)-2}{s+4}}, \tag{7}$$

$$S_m \propto r^{-\frac{5b+2s(a-1)+3a-13}{s+4}}. \tag{8}$$

Therefore, applying the above expressions for the rising phase of the outbursts observed in BL Lacertae ($s = 1.3$, $a_1 = -0.60$, $b_1 = 1.5$) we obtain $a = 2.0$ and $b = -0.71$. This value of b implies that the acceleration of electrons is much more effective than the adiabatic acceleration ($b = +2(s+2)/3 = +2.2$), leading $K \propto r^{0.71}$ to increase with r (or t) during the rising phase. For the decay phase ($a_3 = -2.11, b_3 = -2.28$), we obtain $a = 2.0$ and $b = 3.31$. Interestingly, the value of parameter a derived for the decay phase is the same as that for the rising phase, but the value for parameter b implies that the density of the relativistic electrons $K \propto r^{-3.31}$, which decreases with r much faster than in the case of the adiabatic expansion jet ($b = +2.2$).

We point out that Stevens et al. (1996) obtained similar results in their study of the evolution of radio–mm outbursts in the quasar 3C345: parameter $a = 0.5$ and parameter $b = 4.5$ for the decay phase of the 1991 – 2 outburst ($s = 2$). Since $a < 1$ and b is larger than that for pure adiabatic expansion, they conclude that even during the decay phase, field magnification and radiative losses exist. The value of b obtained from the analysis is much larger than that expected for an adiabatic flow where $b = 2(s+2)/3 = 8/3$ ($s = 2$). In this case, the assumption that the jet is adiabatic (2-dimensional) is possibly not justified. The most probable explanation is that the radiative (synchrotron and inverse-Compton) losses suffered by the electrons have a significant effect on the jet energetics. A value of $a < 1$ suggests that the field is undergoing regeneration due to turbulent processes (Hughes et al. 1989a,b).

We have also examined the rising phase of the outbursts in 3C345 and found $a = 1.2$ and $b = 0.73$; both are quite different from those derived for the decaying phase.

Similar results are also found for outbursts observed in 3C273 (Stevens et al. 1998), which show that more effective mechanisms for electron acceleration and field acceleration (in comparison with the adiabatic acceleration and magnification mechanism assumed in Marscher & Gear's model) could fit the 3-stage evolution of cm–mm outbursts in blazars.

These results show that to explain the evolution of radio–mm outbursts in blazars, some mechanisms for electron acceleration and field magnification should be introduced to describe the evolution of the shock. However, assuming both a and b as free parameters seems to be a bit too arbitrary.

5 A NEW MODEL

As shown by the model fitting of the cm–mm outbursts of BL Lacertae in the previous section, we find that the evolution of the outbursts is caused by injection of relativistic electrons, a magnetic field and adiabatic expansion of the shocked plasma. Even in the growing phase, Compton–synchrotron losses are not significant. Thus, we consider a new model. The rising phase is considered to be related to the rapid injection of electrons and amplification of the magnetic field by the shock and the thickness of the shocked plasma region rapidly increases with respect to the jet radius. Only the adiabatic expansion regime is considered and radiative losses due to Compton and synchrotron radiation do not dominate. That is, we will assume that the thickness of the shocked plasma x_m (or x) is described by the following expression:

$$x_m(\text{or } x) \propto r^q, \tag{9}$$

where index q may have different values for the 3 stages, in particular having a large value for the growth phase.

Therefore, the evolution of cm–mm outbursts can be described as:

$$S_m \propto r^{\frac{-(3s+2)-(3+2s)a+5q}{s+4}} \delta^{\frac{3s+7}{s+4}}, \tag{10}$$

$$\nu_m \propto r^{\frac{-2(s+2)-(s+2)a+2q}{s+4}} \delta^{\frac{s+2}{s+4}}, \tag{11}$$

and

$$S_m \propto \nu_m^{\frac{(3s+2)+(3+2s)a-5q}{2(s+2)+(s+2)a-2q}} \delta^{\frac{3s+7}{s+2}}. \tag{12}$$

In principle, when the spectral evolution of optical/radio outbursts is investigated, both intrinsic variation and the variation of the Doppler factor (δ) of the emitting region along the jet should be considered. For example, Qian et al. (1996c) studied the intrinsic evolution of the superluminal component C4 of 3C345 with its beaming factor variation being taken into account. In the study of the spectral evolution of the IR–mm flare in 3C273, Qian et al. (1999a) and Qian (1999b) also considered the bulk acceleration of the flaring component at its rising (Compton) stage in order to improve the fit of the spectral evolution at lower frequencies. However, beaming is an achromatic effect and a simple change in the Doppler factor cannot explain the spectral evolution of outbursts. Spectral evolution is mainly caused by intrinsic effects. Thus, in the following we will ignore the effects caused by the variation of the Doppler factor ($\delta = \text{constant}$) and only concentrate on the effects due to acceleration/injection of relativistic electrons and field amplification.

We will try to derive the parameters (a, q) to fit the the variability pattern (S_m-ν_m relation) observed in BL Lacertae (assuming $r \propto t$ – observing time).

5.1 Derivation of Parameters a and q

As is well known, the plateau phase is a very short period and, in some sources, this phase has not been verified (Stevens et al. 1998, 1996, 1995; Litchfield et al. 1995). In our case, this phase and the parameters (a_2, b_2) have not been well defined. So, we concentrate on discussion of the growth and decay phases.

– For the decay phase we have the equations:

$$-(3s+2)-(2s+3)a+5q=(s+4)b_3, \tag{13}$$

and

$$-2(s+2)-(s+2)a+2q=(s+4)a_3. \tag{14}$$

Substituting $a_3=-2.11$, $b_3=-2.28$ and $s=1.3$ into Equations (15) – (16), we find $a=2$ and $q=1$. In this case, we have: $S_m \propto r^{-\frac{7s+3}{s+4}}$ and $\nu_m \propto r^{-\frac{4s+6}{s+4}}$, which is completely similar to the decay phase governed by a 3-dimensional spherical adiabatic expansion with the total magnetic field flux being conserved ($B_* \propto r^{-2}$).

– For the growth (or rising) phase, we should substitute $a_1=1.50$ and $b_1=-0.60$ into the above Equations (15) – (16) instead of a_3 and b_3. In this case, we find $a=2$ (interestingly, exactly the same value as for the decay phase) and $q=5$. The consistency of the derived parameter value of a between the growth and decay phase seems rather significant, implying that during both the rising and decay phases, the magnetic field is basically longitudinal along the jet and its strength is proportional to r^{-2}. However, unlike $q=1$ for the decay phase, for the growth (rising) phase q = 5, implying that during the growth (rising) phase, the size of the shocked plasma along the line of sight rapidly increases with r (x_m(or x) $\propto$ r^5).

– After the derivation of the parameters a and q for both growth and decay phases, we would suppose that for the outbursts observed in BL Lacertae, a continuous change of the parameter q from $q=5$ to $q=1$ may be able to explain the plateau stage (transitional phase between growth and decay phases). In fact, in this case the power law index of the S_m-ν_m relation ($S_m \propto {\nu_m}^{\epsilon}$) is (from Eqs. (12) and (13)):

$$\epsilon=-\frac{5q-(2s+3)a-(3s+2)}{2(s+2)+(s+2)a-2q}. \tag{15}$$

Thus, for $q=4$, 3 and 2 (note: $a=2$ and $s=1.3$), we obtain $\epsilon=-0.55$, +0.29 and +0.77 respectively. These values indeed show the transition from the growth phase ($q=5$, $\epsilon=-1.50$) to the decay phase ($q=1$, $\epsilon=+1.08$). Therefore, we have shown that the solutions obtained for a and q ($a=2$ and q vary from $q=5$ to $q=1$) can adequately interpret the 3-stage evolutional behavior of the cm–mm outbursts observed in BL Lacertae.

5.2 Comparison with Outbursts in other Blazars

Before we discuss the physical implications of the results obtained in the last section (x_m (or x) $\propto$ r^5) for the growth phase, we first check whether this procedure could also be applied to the outbursts observed in other blazars. As examples, we consider the cm–mm outbursts observed in the two blazars: 3C273 and 3C345.

– 3C273: Stevens et al. (1998) studied the evolution of the centimeter–submillimeter outburst of 3C273 during the period (1995.11.13 – 1996.06.01). The quiescent-subtracted (flare) spectra are well fitted by a homogeneous synchrotron curve to derive the values of parameters (S_m, ν_m) and the optically thin spectral index α (energy index $s=2\alpha$+1). Interestingly, they obtain $s=2.0$ for all the three phases, having no significant change from the growth to the decay phase. They also found that for the growth phase of the outburst observed in August 1995 $a_1=-0.75$ (the epoch at which the flare began is taken to be $t_0=1995.07.18$) and $b_1/a_1=-1.5$ ($b_1=1.13$). Substituting these numbers into Equations (15) and (16), we obtain $a=2.0$ and $q=5.75$ for the growth phase. In the paper, they did not give the values (a_3 and b_3) and (a, q) cannot be determined directly. If $a=2$ and $q=1$ are assumed for the decay phase, we obtain $a_3=-2.3$ and $b_3=-2.8$ ($\epsilon=1.2$: $S_m \propto {\nu_m}^{1.2}$) which are approximately consistent with the observations given in their figure 8 (Stevens et al. 1998). In the case of 3C273, our modeling result $a=2$

implies that the magnetic field is aligned along the jet axis, which is unexpectedly consistent with the VLBI polarization observations: during the 1995 flare, the 270 GHz polarization was 6% – 7% and the electric field vector was observed to be perpendicular to the VLBI jet axis. At centimeter wavelengths (e.g. 14.5 GHz) the polarization position angle also suggests that the electric vector is aligned perpendicular to the VLBI jet structural axis, similar to what was found at millimeter wavelengths (Stevens et al. 1998). The consistency of our fitting results with the VLBI polarization observations once again prove the validity of our model.

– 3C345: Stevens et al. (1996) studied the evolution of the centimeter–submillimeter spectrum of 3C345 during 1991.04.20 – 1993.08.15. This outburst comprised one growth phase and two decay phases. They found that after the substraction of the underlying quiet level, the flare spectrum is well fitted by a homogeneous synchrotron curve. The evolution of turnover frequency (ν_m) with turnover flux (S_m) is compared with the predictions of the MG shocked-jet model. They found that a power-law is a remarkably good approximation to the observed trend. The turnover moves smoothly towards lower frequencies with time as expected from an emitting region that is expanding. The turnover flux initially rises and then decays with an index of ~ 1.0. This decay is interrupted by a second rise which also decays with an index of ~ 1.0. (The second rise leads to a broad peak and flatter ν_m values decrease with time). The implied magnetic field orientation is parallel to the shock front (perpendicular to the jet axis) as expected from compression of the underlying turbulent (random) field. The observed rise of S_m with ν_m is inconsistent with both the synchrotron and Compton phases of the MG model and may be related to the mechanisms responsible for the shock formation (and evolution of the emitting region). From the light curves given in that paper, we found that for the parameters (S_m and ν_m) given in their table 1, only the values which are obtained from the homogeneous synchrotron curve fits the flare spectra measured at epochs–1 (1991.04.20) and –2 (1991.06.10) are actually attributed to the growth phase. The values of (S_m and ν_m) obtained for the other four epochs are measured at the broad peaks of the outburst and cannot be used to determine the behavior of the growth phase. Thus, we use the values of S_m and ν_m for the two epochs to determine $a_1 = -0.69$ and $b_1 = 0.86$ ($S_m \propto {\nu_m}^{-1.24}$. Note that the starting epoch of the outburst is at 1990.09.01, thus $t_1 = 235$ d, $t_2 = 285$ d). Then, using Equations (15) and (16) ($s = 2.0$), we obtain $a = 1.2$ and $q = 4.3$ for the growth phase. Correspondingly, if we assume that the decay phase has $a = 1.2$ and $q = 1$, $\epsilon = +1.0$ is derived, almost exactly equal to the value +0.98 derived by Stevens et al. (1996) for the decay phase ($S_m \propto {\nu_m}^{0.98}$).

Through this comparison, we find that for the three blazars (BL Lacertae, 3C273 and 3C345) the derived values for parameter a ($B \propto r^{-a}$) are in the range of 1 to 2, which is consistent with those usually assumed in shocked jet models, corresponding to two extreme regimes of the magnetic field in jets: a pure longitudinal and pure transverse field. Also, the derived values for the parameter q (x_m (or x) $\propto r^q$) are in the range of ~ 4 to 6 for the growth phase, implying that the size of the synchrotron emitting region along the line of sight (with respect to the radius (r) of the jet) increases very rapidly due to the injection of electrons and the magnetic field by the shock.

The consistency between the values of (a, q) derived for the growth phases in three blazars may imply that our model can be generally applied to interpret the evolution of cm–mm outbursts observed in blazars. In other words, the behavior of cm–mm outbursts can be explained in terms of the 3-stage evolution model proposed in this paper with parameter q changing from $\sim$5 (growth phase) to $\sim$1 (decay phase).

5.3 Summary

The results of our model-fitting of the cm–mm outbursts of BL Lacertae can be described as follows:

– (1) The outbursts at 90 – 350 GHz varied simultaneously, and their time-lags relative to the associated optical flares were in the range of $\sim 80 - 100$ d. The outbursts were optically thin

from the beginning and the flux peaks construct a spectrum with a spectral index of ~ 0.15. Moreover, there is no change in the spectral index throughout the outbursts, and thus the rising phases of the outbursts are not related to Compton or synchrotron radiative losses.

– (2) The timelags shown in Figures 11 and 12 indicate that only at lower frequencies (37, 22, 15, 8 and 4.8 GHz) does the timelag gradually increase with decreasing frequency, showing that the outbursts at these low frequencies are optically thick at the beginning and gradually become optically thin with time.
– (3) Our new 3-stage evolutional model (shock-in-jet model) can explain the evolution of the cm–mm outbursts of BL Lacertae well and has been proved valid for the outbursts in other blazars (3C273 and 3C345). The most impressive results are that the power index a for the magnetic field derived for the growing and decay phases is consistent and is also proved to be valid by VLBI polarization observations. More tests on the evolution of cm–mm outbursts of more blazars would be very helpful. The key point of our model is the assumption that the growing phase of the cm–mm outbursts is produced by the rapid injection of relativistic electrons and a magnetic field by a shock in a highly collimated jet. The decay phase occurs when the injection ends and the shocked plasma enters into a 3-dimensional adiabatic expansion (transition from a highly collimated regime to a, for example, conical expansion regime). The plateau phase is a short transitional phase which cannot be clearly defined.

6 DISCUSSION: PHYSICAL IMPLICATIONS

We have proposed a new model to interpret the cm–mm outbursts in BL Lacertae in terms of the 3-stage evolution model, which can also be applicable to cm–mm outbursts observed in 3C273 and 3C345. In our model, the key parameter which controls the evolution is q. When q varies from $q \simeq 5$ to $\simeq 1$, the outbursts evolve from the rising phase to the decay phase. What mechanism can cause such a variation of q?

Firstly, we need to explain the relation $x_m \propto r^5$ for the growth phase.

As is well known, in relativistic shock models, the magnetized plasma containing the relativistic electrons accelerated by the shock front moves away from the shock front (towards the downstream direction of the shock with a velocity of $\sim 0.3c$; see, e.g., Mastichiadis & Kirk 1997). In the case of cm–mm outbursts where radiation losses (Compton and synchrotron loss) are assumed to be not significant, the extent or the size of the shocked plasma along the jet (i.e. x) can thus be assumed to be proportional to the distance d of the shock front from the jet apex. Therefore, $x \propto r^q$ implies that $d \propto r^q$. In this case, $q \simeq 5$ for the growth phase implies that the rising (growth) phase of the outbursts occurs in highly collimated regions of the jet, for example, in regions described by parabolic forms ($d \propto r^p$, $p > 5 - 6$). This is in contrast to the conical-jet assumption which is usually assumed in shocked jet models (for example, see Marscher & Gear 1985). This explanation also shows that the requirement of rapid injection of relativistic electrons and a magnetic field can be satisfied for the growth phase if the jet is highly collimated. This solves the inherent difficulties (excessive acceleration and field amplification) for the plasmon (spherically expanding) models discussed by Marscher & Gear (1985, see the Appendix of their paper).

Moreover, our model also provides a plausible approach to accommodate the simple expanding source model (van der Laan 1966; Pauliny-Toth & Kellermann 1966) within the shocked jet models (Kellermann 2003). That is, in the frame of our model, $q \simeq 1$ for the decay phase indicates that the shocked plasma has reached a point where the injection of electrons and a magnetic field ends and the jet suddenly opens sideways and completely leaves the collimated region, entering a new stage of 3-dimensional adiabatic expansion. Obviously, the plateau stage corresponds to a transitional phase between the growth phase with $q \simeq 5$ (collimated jet region) and the decay phase with $q \simeq 1$ (3-dimensional expanding plasmon). Geometrically, this transitional region may be regarded as the structure of the jet changing from a highly collimated shape to a broadly conical shape. During this

process, the bulk speed of the emitting plasma could change, as suggested by Daly & Marscher (1988) and Krichbaum et al. (1990b).

Acknowledgements This research has made use of data from the University of Michigan Radio Astronomy Observatory which is supported by funds from the University of Michigan and by a series of grants from the NSF. This paper is partly based on observations carried out at the 30 m telescope of IRAM, which is supported by INSU/CNRS (France), MPG (Germany) and IGN (Spain).

This work was started when SJQ visited the Max-Planck-Institut für Radioastronomie in 2005. SJQ gratefully acknowledges the hospitality and the financial support from the MPIfR.

References

Aller, M. F., Aller, H. D., Hughes, P. A., & Latimer, G. E. 1999, ApJ, 512, 601

Aller, M. F., Aller, H. D., & Hughes, P. A. 2003, in ASP Conf. Ser. 300, Radio Astronomy at the Fringe, eds. J. A. Zensus, M. H. Cohen, & E. Ros, 159

Balonek, T. J. 2004, BAAS, 36, 1600

D'Arcangelo, F. D., Marscher, A. P., Jorstad, S. G., et al. 2007, ApJ, 659, L107

Daly, R. A., & Marscher, A. P. 1988, ApJ, 334, 539

Hughes, P. A., Aller, M. F., & Aller, H. D. 1985, ApJ, 298, 301

Hughes, P. A., Aller, H. D., & Aller, M. F. 1989, ApJ, 341, 54

Hughes, P. A., Aller, H. D., & Aller, M. F. 1989, ApJ, 341, 68

Jorstad, S. G., Marscher, A. P., Stevens, J. A., et al. 2007, AJ, 134, 799

Kellermann, K. I. 2003, in ASP Conf. Ser. 300, Radio Astronomy at the Fringe, eds. J. A. Zensus, M. H. Cohen, & E. Ros, 185

Kellermann, K. I., & Pauliny-Toth, K. K. I. 1969, ApJ, 155, L71

Krichbaum, T. P., Booth, R. S., Kus, A. J., et al. 1990a, A&A, 237, 3

Krichbaum, T. P., Hummel, C. A., Quirrenbach, A., et al. 1990b, A&A, 230, 271

Krichbaum, T. P., Kraus, A., Otterbein, K., Britzen, S., & Witzel, A. 1998, in ASP Conf. Ser. 144, Radio Emission from Galactic and Extragalactic Compact Sources (IAU Colloquium 164), eds. J. A. Zensus, G. B. Taylor, & J. M. Wrobel, 37

Litchfield, S. J., Stevens, J. A., Robson, E. I., & Gear, W. K. 1995, MNRAS, 274, 221

Marscher, A. P., & Gear, W. K. 1985, ApJ, 298, 114

Marscher, A. P. 2005, MmSAI, 76, 13

Marscher, A. P. 2008, in ASP Conf. Ser. 386, Extragalactic jets: Theory and Observation from Radio to Gamma Ray, 437

Mastichiadis, A., & Kirk, J. G. 1997, A&A, 320, 19

O'Dell, S. L., Dennison, B., Broderick, J. J., et al. 1988, ApJ, 326, 668

Pacholczyk, A. G. 1970, Radio Astrophysics (San Francisco: Freeman)

Pacholczyk, A. G., & Scott, J. S. 1976, ApJ, 210, 311

Pauliny-Toth, I. I. K., & Kellermann, K. I. 1966, ApJ, 146, 634

Peterson, F. W., & Dent, W. A. 1973, ApJ, 186, 421

Qian, S. J. 1996a, Chin. Astron. Astrophy., 20, 137 (or AcApS 16, 15)

Qian, S. J. 1996b, Chin. Astron. Astrophy., 20, 281 (or AcApS 16, 143)

Qian, S. J., Krichbaum, T. P., Zensus, J. A., Steffen, W., & Witzel, A. 1996c, A&A, 308, 395

Qian, S. J. 1997, Acta Astronomica Sinica, 38, 239

Qian, S. J., Zhang, X. Z., Witzel, A., Krichbaum, T. P., Britzen, S., & Kraus, A. 1998a, in ASP Conf. Ser. 144, Radio Emission from Galactic and Extragalactic Compact Sources (IAU Colloquium 164), eds. J. A. Zensus, G. B. Taylor, & J. M. Wrobel, 93

Qian, S. J., Zhang, X. Z., Witzel, A., Krichbaum, T. P., Britzen, S., & Kraus, A. 1998b, Chin. Astron. Astrophy., 22, 155 (or AcApS 18, 17)
Qian, S. J., Witzel, A., Krichbaum, T. P., Kraus, A., Zensus, J. A., & Zhang, X. Z. 1999a, in ASP conf. Ser. 159, BL Lac Phenomenon, eds. L. O. Takalo, & A. Sillanpää, 443
Qian, S. J. 1999b, Chin. Astron. Astrophy., 23, 166
Rabaça, C. R., & Zensus, J. A. 1994, in Compact Extragalactic Radio Sources, eds. J. A. Zensus, & K. I. Kellermann (Green Bank: NRAO), 163
Stevens, J. A., Litchfield, S. J., Robson, E. I., Hughes, D. H., Gear, W. K., Teräsranta, H., Valtaoja, E., & Tornikoski, M. 1994, ApJ, 437, 91
Stevens, J. A., Litchfield, S. J., Robson, E. I., Gear, W. K., Teräsranta, H., Tornikoski, M., & Valtaoja, E. 1995, MNRAS, 275, 1146
Stevens, J. A., Litchfield, S. J., Robson, E. I., Cawthorne, T. V., Aller, M. F., Aller, H. D., Hughes, P. A., & Wright, M. C. H. 1996, ApJ, 466, 158
Stevens, J. A., Robson, E. I., Gear, W. K., Cawthorne, T. V., Aller, M. F., Aller, H. D., Teräsranta, H., & Wright, W. C. H. 1998, ApJ, 502, 182
Stirling, A. M., Cawthorne, T. V., Stevens, J. A., et al. 2003, MNRAS, 341, 405
Teräsranta, H., Wiren, S., Koivisto, P., Saarinen, V., & Hovatta, T. 2005, A&A, 440, 409
Ungerechts, H., Kramer, C., Lefloch, B., et al. 1998, in ASP Conf. Ser. 144, Radio Emission from Galactic and Extragalactic Compact Sources (IAU Symposium 164), eds. J. A. Zensus, G. B. Taylor, & J. M. Wrobel, 149
Valtaoja, E., Haarala, S., Lehto, H., Valtaoja, L., Valtonen, M., Moiseev, I. G., Nesterov, N. S., Salonen, E., Teräsranta, H., Urpo, S., & Tiuri, M. 1988, A&A, 203, 1
Valtaoja, E., Teräsranta, H., Urpo, S., Nesterov, N. S., Lainela, M., & Valtonen, M. 1992, A&A, 254, 71
van der Laan, H. 1996, Nature, 211, 1131
Villata, M., Raiteri, C. M., Kurtanidze, O. M., et al. 2004a, A&A, 421, 103
Villata, M., Raiteri, C. M., Aller, H. D., et al. 2004b, A&A, 424, 497
Villata, M., Raiteri, C. M., Balonek, T. J., et al. 2006, A&A, 453, 817